

Surface-modified 3D scaffolds for tissue engineering

R. F. S. LENZA*, W. L. VASCONCELOS

Federal University of Minas Gerais, Department of Metallurgical and Materials Engineering
Rua Espírito Santo, 35 - 2^o andar -30160-030, Belo Horizonte, MG, Brazil

J. R. JONES, L. L. HENCH

Imperial College of Science, Technology and Medicine, Centre for Tissue Engineering and Repair, Department of Materials, Prince Consort Road, London SW7 2BP, UK
E-mail: rulenza@zipmail.com.br

The aim of this work was to use sol–gel processing to develop bioactive materials to serve as scaffolds for tissue engineering that will allow the incorporation and release of proteins to stimulate cell function and tissue growth. We obtained organofunctionalized silica with large content of amine and mercaptan groups (up to 25%). The developed method can allow the incorporation and delivery of proteins at a controlled rate. We also produced bioactive foams with binary SiO₂–CaO and ternary SiO₂–CaO–P₂O₅ compositions. In order to enhance peptide–material surface properties, the bioactive foams were modified with amine and mercaptan groups. These materials exhibit a highly interconnected macroporous network and high surface area. These textural features together with the incorporation of organic functionally groups may enable them to be used as scaffolds for the engineering of soft tissue.

© 2002 Kluwer Academic Publishers

1. Introduction

Tissue engineering is a multidisciplinary field that uses the principles of engineering and life science in the development of biological substitutes that create new tissues and restore, maintain or improve tissue function [1–2]. A number of tissue engineering strategies have been developed, and some involve the transplantation of cells on or within bioactive matrices [2]. This approach is based on the natural ability of the living cells to regenerate damaged tissue. The preparation of tissues *in vitro* can start from isolated cells harvested from the patient or from a donor. These cells can then be seeded on bioactive substrates and cultured *in vitro* for tissue formation before being implanted at the damaged site. Such tissue may offer an alternative to organ transplantation [1, 3]. It is hoped that these “bioartificial” organs will be able to carry out complex biochemical functions and to regenerate as normal tissue [4–5].

Biomaterials with specific proteins grafted on the surface can potentially control and facilitate tissue formation or regeneration. Biocolonization of scaffold surfaces is probably one of the main approaches for promoting interactions between biomaterials and tissues. Biocolonization involves attachment and differentiation of tissue cells on the surface of a biomaterial [6]. In order to ensure proper development of the desired tissue, it is necessary to have a complete understanding of cellular interactions with bioactive materials and their potential

to impact tissue formation [4–5]. The biocompatibility and biocolonization of biomaterials is affected by the adsorption of proteins onto the surface of the materials. The chemical functionality and texture of the material surface must be tailored for successful protein attachment. Such attachment must not denature the proteins, so that recognition between cells of the tissue and adsorbed proteins is not inhibited [6]. To modify biomaterial surfaces, proteins may be either adsorbed or covalently grafted to the surface [7] or included in the bulk composition [8].

Sol–gel technology allows the introduction of functional biomolecules into the material network. In addition, sol–gel materials exhibit high surface areas and very porous structures which provide numerous sites for cell–material interactions [6]. New developments in sol–gel technology have allowed preparation of materials with a wide range of physical and chemical properties. [6, 9–11]. It has been shown by previous work [6, 9] that sol–gel matrices modified with organic functional groups can be used to successfully incorporate certain proteins and release them at a controlled rate. The presence of amine and mercaptan groups on the biomaterials surfaces yield patterns of chemical activity that can be useful to encourage interaction of the inorganic substrate with specific proteins. Mansur *et al.* [6] showed that incorporation mercaptan and amine groups into silica gel networks allowed attachment of proteins such as

*Author to whom all correspondence should be addressed.

bovine serum albumin and pork insulin. Pork insulin attached preferentially to mercaptan groups, due to the more hydrophobic of the insulin, whereas the more hydrophilic albumin preferentially attached to the amine. The results showed that creation of chemically patterned surfaces can favor or reduce interactions between surfaces and well-organized macromolecules such as proteins.

Recently, sol-gel derived bioactive glasses of various compositions have been foamed to produce resorbable macroporous 3D scaffolds with high potential for bone regeneration. These scaffolds exhibit a hierarchical structure comprised of an interconnected macroporous network and mesoporous texture [12]. The macroporous network has the potential to allow tissue ingrowth and vascularisation. The mesoporous texture (pore diameters in the range of 2–50 nm) provides a high surface area for enhanced ion release and bioactivity on contact with body fluid.

This paper describes the synthesis and characterisation of sol-gel derived biomaterials for use as a scaffold for tissue engineering and as a carrier for biologically active molecules. The compositions studied were macroporous bioactive glass foams in the binary $\text{SiO}_2\text{-CaO}$ (70S30C) [13] and ternary $\text{SiO}_2\text{-CaO-P}_2\text{O}_5$ (58S) [14] compositions and hybrid organic/inorganic silica gel-glass monoliths, obtained by a modified acid alkoxide route to allow the incorporation of bioactive molecules. In order to enhance protein-material surface properties, the bioactive foams were modified with amine and mercaptan groups.

2. Experimental

2.1. Organofunctionalized silicas

Organomodified silicas were prepared by co-polymerization of tetraethoxysilane (TEOS, Aldrich) and the organosilanes- γ -aminepropyltriethoxysilane (APTS, Aldrich) or mercaptopropyl-trimethoxysilane (MPTS, Aldrich), using a single-step acid catalyzed process [11]. TEOS, APTS or MPTS, H_2O and 1N HNO_3 (Merck) with molar ratios $1 - x : x : 4 : 1.0 \times 10^{-3}$, where x ranged from 2.5 to 25 mol %, were mixed at 20 °C under stirring. The sols were cast into cylindrical plastic containers and heat-treated at 60 °C for 48 h.

2.2. Bioactive foams

The binary 70% SiO_2 -30% CaO (70S30C) and the ternary 60% SiO_2 -36% CaO -4% P_2O_5 (58S) gel-glasses were prepared by the sol-gel method, which involved mixing distilled water, the appropriate alkoxide precursors and salts, and nitric acid (the catalyst for hydrolysis). On completion of hydrolysis, the sols were foamed by vigorous agitation with the aid of surfactant, distilled water and 0.1 wt % HF as a catalyst for the condensation reaction. The surfactant stabilized bubbles formed early in the foaming process, then as the polycondensation reaction continued, viscosity increased. As viscosity began to rise more steeply the foam was poured into molds and sealed for gelling, during which the bubbles become permanently stable.

The materials were aged at 60 °C for 48 h, dried at 130 °C for 48 h and stabilized at 600 °C for 20 h [12].

Before surface modification the stabilized foams were degassed under vacuum at 200 °C for 20 h to eliminate water molecules and other residues. Surface modification was carried out by soaking 0.10 g of foams in a solution containing 10 mL of dry toluene and 0.5 mL of APTS or MPTS at 37 °C for 5 h under constant agitation. The silanized foams were withdrawn from the solution and washed with toluene to remove any unreacted organosilanes. The modified-biomaterials were then heat-treated at 80 °C for several hours to eliminate any trapped toluene.

2.3. Characterization

An Autosorb AS-6 (Quantachrome) instrument was used to obtain N_2 sorption isotherms of the materials after outgassing at 130 °C for 4 h. The specific surface area was calculated from BET analysis [12] using the linear region between $0.05 < P/P_0 < 0.20$ that gave a least-square correlation $R^2 > 0.9999$. The N_2 molecular cross-sectional area was assumed to be 0.162 nm^2 . The pore volume was calculated from the high P/P_0 portion of the isotherm where the volume of N_2 adsorbed was constant. The pore radii distribution was calculated by the BJH method applied to desorption curves [15]. The experimental error was $< 10\%$.

The macroporous network was analyzed using mercury intrusion porosimetry (PoreMaster33, Quantachrome). Morphological and textural properties of the biomaterials were analyzed using scanning electron microscopy (JEOL, JMS T220A), with an acceleration potential of 15 KeV, on samples sputter coated with Au.

The molecular structure of the materials was investigated by Fourier transform infrared spectroscopy (FTIR). Spectra were collected using a Mattson Genesis II spectrometer with a Pike Technologies EasiDiff diffuse reflectance accessory in the range $400\text{-}4000 \text{ cm}^{-1}$ using 2 cm^{-1} resolution and 128 scans. A sample to KBr ratio of 1 : 100 was necessary to avoid spectral reflectance.

3. Results

3.1. Organofunctionalized silicas

N_2 adsorption-desorption isotherms of the hybrid organic/inorganic silicas are shown in Fig. 1. These were type IV isotherms, according to the BDDT classification originally proposed by Brunauer and co-workers, which are characteristic of mesoporous (2–50 nm pore diameter) materials [16]. The isotherms exhibit type H2 hysteresis loops in the mesoporous range, which is characteristic of the so-called ink-bottle pores that have pore cavities larger in diameter than the openings (throats) leading into them [17–20]. Fig. 1 shows that less gas is adsorbed for hybrid silica compared to pure silica, and the amount of adsorption decreased with an increase in the organic molar fraction. Specific surface area (S_p), specific pore volume (V_p) and average pore radius (r_p) for the pure silica and hybrid materials are presented in Table I. Specific surface area, pore volume and average pore size also decreased with

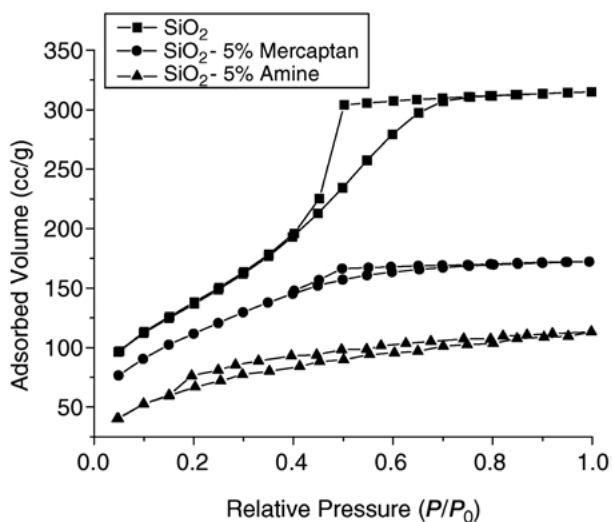


Figure 1 Nitrogen adsorption-desorption isotherms of pure silica and organofunctionalized silica: (■) pure silica, (●) silica with 5% of mercaptan groups and (▲) silica with 5% amine groups.

TABLE I Textural properties of organofunctionalized silica

| Sample | S_p (m ² /g) | V_p (cc/g) | R_p (nm) | C |
|---------------|---------------------------|--------------|------------|-----|
| Pure silica | 516 | 0.53 | 3.8 | 50 |
| 2.5% amine | 503 | 0.33 | 2.6 | 52 |
| 5% amine | 500 | 0.32 | 2.5 | 83 |
| 10% amine | 302 | 0.18 | 2.3 | 112 |
| 5% mercaptan | 413 | 0.27 | 2.6 | 61 |
| 10% mercaptan | 384 | 0.19 | 2.3 | 175 |
| 25% mercaptan | 338 | 0.21 | 2.4 | 373 |

the increase in the organic fraction. These results suggest that as organic fraction increased, the pores filled with organic chains and the amount of adsorption, specific surface area, pore volume and pore size all decreased. As shown in Table I, C constants, from the BET analysis, for the materials with higher organic molar fractions are much larger than that for the pure silica, due to changes in the material composition.

Fig. 2 shows the FTIR spectra of the pure silica and silica with 5% of APTS and 5% MPTS. The spectrum of pure silica exhibits the characteristic SiO₂ band at

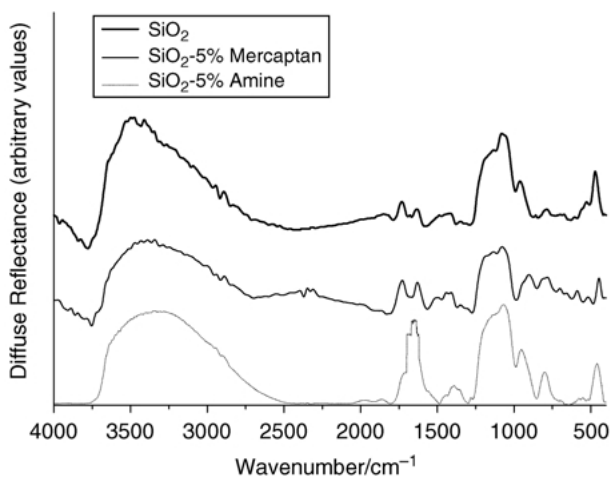


Figure 2 FTIR spectra of pure silica and organofunctionalized silica.

1000–1100 cm⁻¹, associated with the antisymmetric Si–O stretching vibration involving bridging Si–O–Si oxygen, and the band at 400–600 cm⁻¹ which is the complementary bending (or rocking) vibrations of the network due to Si–O–Si bonds and Si–OH bonds (3500 and 950 cm⁻¹) [21]. The spectrum in Fig. 2(b) is from the silica gel modified with 5% with MPTS and the spectrum in Fig. 2(c) is from silica with 5% of APTS. These spectra exhibit peaks at 2450–2550 and 680 cm⁻¹ that are characteristic of the mercaptan vibrational modes and at 1570–1580 cm⁻¹ that are characteristic of the vibrational modes of the amine groups, respectively [8]. These results demonstrate that the experimental procedure used in this work was successful in altering the chemistry of silica-based gels.

3.2. Bioactive foams

Fig. 3(a) shows the macrostructure of the foams before surface modification. The foams exhibit an interconnected 3D structure with very large pores and large interconnects between them. Both 70S30C and 58S foams have interconnecting pore systems with pores of sizes up to 600 μm.

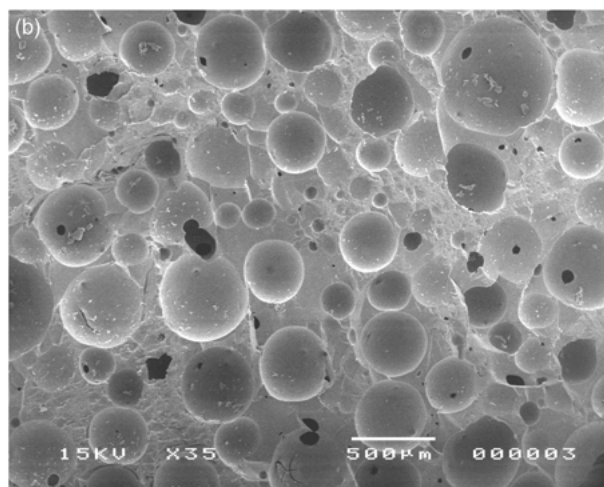
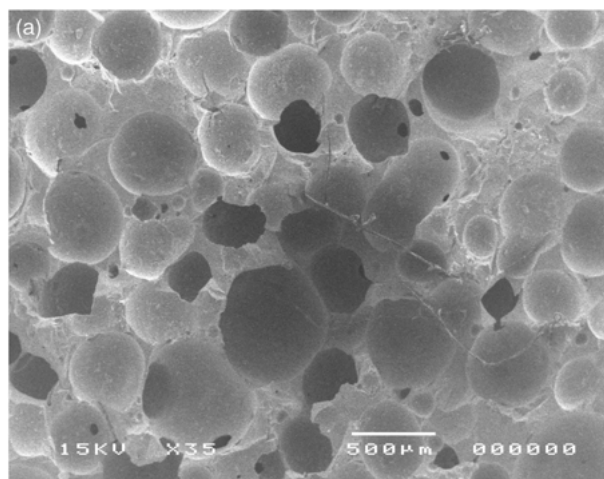


Figure 3 SEM micrographs of bioactive foams: (a) 70S30C foam, (b) 70S30C foam modified with amine group and (c) 70S30C modified with mercaptan group.

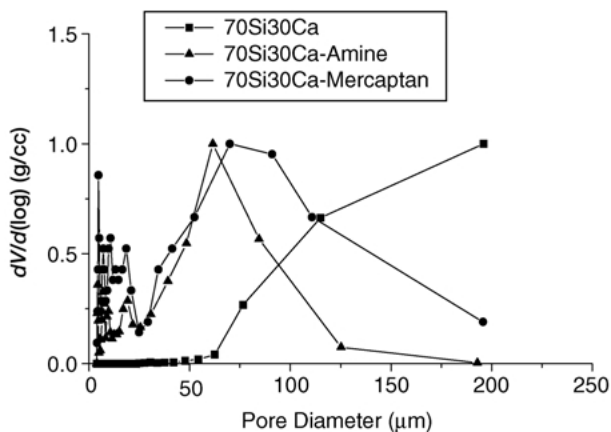


Figure 4 Mercury porosimetry curves for bioactive foams: (■)70S30C foam, (●) 70S30C foam modified with mercaptan group and, (▲)70S30C modified with amine group.

Fig. 3 (b) shows the macrostructure of the foams after modification with the mercaptan group. The surface-modified samples still present a very interconnected macroporous network. While the untreated foams present a very smooth surface, the modified biomaterials exhibit a fine porous texture covering the surface, which is a result of the organic groups immobilized on the surface of the materials.

While the SEM micrographs provided qualitative information on the material structure, mercury porosimetry allowed a quantitative investigation of the porosity of the chemical modified structures. Fig. 4 shows the pore size distribution curves for the materials before and after surface modification. Before modification, the foams exhibited very large pores, with a modal pore diameter greater than $200\ \mu\text{m}$. After modification, the pore size distribution curves are shifted towards small pore sizes and modal pore diameters in the range $60\text{--}70\ \mu\text{m}$. The decrease in the modal pore diameters of foams after chemical modification was caused by the polymerization of the organosilane agents adsorbed on the pores surfaces. The results of Hg porosimetry demonstrate that the foams are highly porous with porosities of $80\text{--}90\%$. As mercury intrusion porosimetry accounts only for pores with sizes $250\ \mu\text{m}$ and smaller and as the SEM images show the samples had pores larger than this critical value we assumed that the true porosity may even be higher. The high porosity and interconnecting pore system presented by these materials can provide diffusion pathways and ample room for protein adsorption and protein delivery.

Table II shows the results of N_2 adsorption–desorption analysis of the foams and bulk density results obtained by mercury porosimetry. The samples exhibited a mesoporous network (average diameter of $3\text{--}23\ \text{nm}$) with a

TABLE II Textural properties of bioactive foams

| Sample | S_p (m^2/g) | V_p (cc/g) | R_p (nm) | C | ρ_b (g/cm^3) |
|--------------------|---------------------------------|--------------------------------|------------|-----|-------------------------------------|
| 70S30C | 155 | 0.89 | 23 | 109 | 0.26 |
| 70S30C – amine | 138 | 0.71 | 22 | 36 | 0.35 |
| 70S30C – mercaptan | 80 | 0.03 | 8 | 4 | 0.28 |
| 58S | 175 | 0.73 | 17 | 171 | 0.24 |
| 58S – amine | 176 | 0.63 | 14 | 33 | 0.32 |
| 58S – mercaptan | 84 | 0.12 | 3 | 4 | 0.33 |

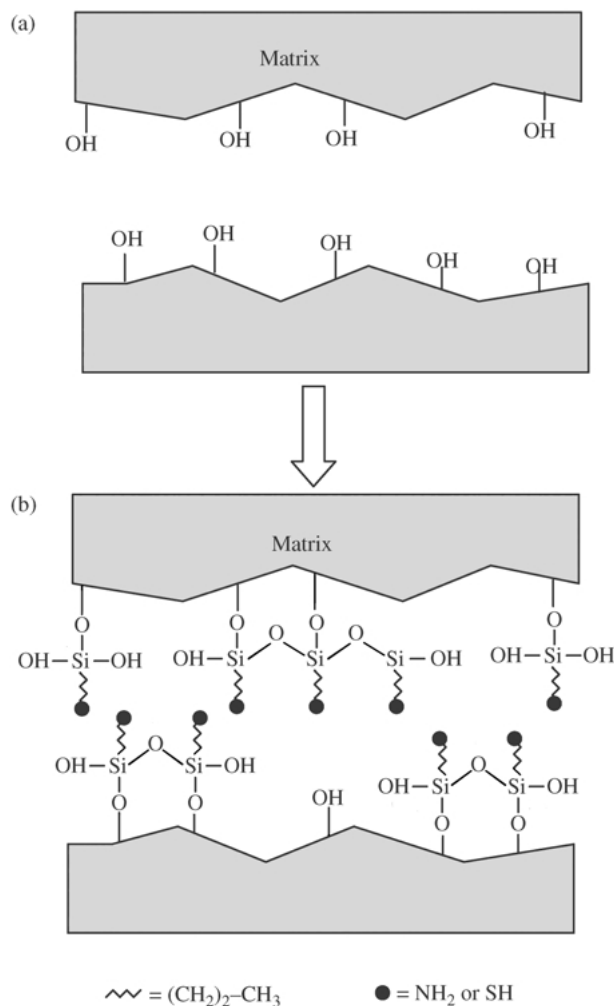


Figure 5 Schematic representation of the pore structure of the surface modified foams: (a) before and (b) after surface modification.

high surface area of $80\text{--}176\ \text{m}^2/\text{g}$. The bulk density of foams increased with surface modification. Consequently, the surface area, specific pore volume and average pore size of foams decreased after modification. This is a consequence of the organic functional groups which covalently bond on the surface of the foams. As shown in Table II, C constants for the surface-modified foams were quite different to that for the original foams. It is known that the C constant is related to heat of adsorption in the BET equation [20]. The difference in C values is therefore thought to be due to a difference in the pore surface. The surface of the original foams was covered with OH (silanol) groups, almost all of which reacted with organosilane compounds and introduced organic groups during surface modification, thus altering the nature of the surface as is schematically shown in Fig. 5.

Fig. 6 shows FTIR spectra of binary silica gels-glasses modified with MPTS and APTS. Spectra of non-modified foams exhibit the characteristic peaks of Si–O stretch ($1100\ \text{cm}^{-1}$), Si–O bending ($600\text{--}400\ \text{cm}^{-1}$), Si–OH peaks ($3500\text{--}950\ \text{cm}^{-1}$) and carbonate peaks at $1500\text{--}1400$, $800\text{--}880\ \text{cm}^{-1}$. The ternary 58S foam also shows phosphate peaks at about 1085 , 960 , $600\text{--}560$ and $460\ \text{cm}^{-1}$ [21] (not shown). After modification the presence of amine ($1580\ \text{cm}^{-1}$) and mercaptan (2550 and $680\ \text{cm}^{-1}$) groups are observed [6]. The organo

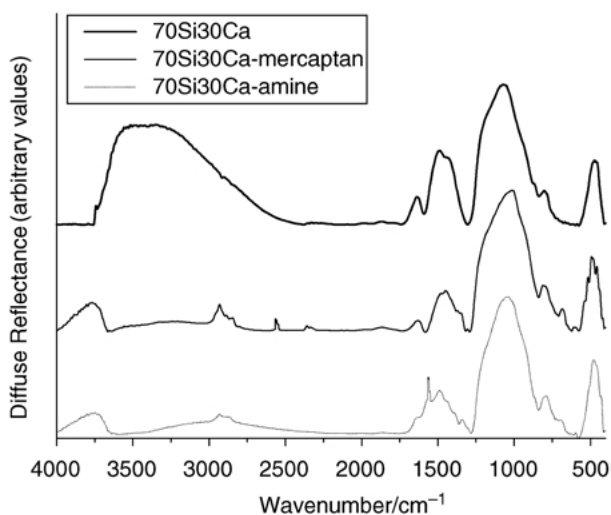


Figure 6 FTIR spectra for bioactive 70S30C foams with and without mercaptan and amine groups.

groups lead to a decrease in intensity of the molecular water peak at $3200\text{--}3600\text{ cm}^{-1}$ and 1640 cm^{-1} and an increase in intensity of the isolated silanol group peak at $3700\text{--}3850\text{ cm}^{-1}$ and the organic groups peak at $2850\text{--}3000\text{ cm}^{-1}$ [19]. These results confirm the successful incorporation of the functional groups on the surface of the foams.

4. Discussion

Inorganic biomaterials have been used as substrates for creating patterned surfaces [6]. In order to alter the chemical properties of the biomaterials towards guiding interactions between proteins and synthetic surfaces, the silica network and foams surface were modified by incorporating amine and mercaptan groups.

Chemically patterned surfaces can control adsorption of proteins in two main ways:

1. Allowing interactions between groups on the protein that resemble (in terms of sequence of chemical affinities) the type of chemical template provided by the surface, thereby affecting the magnitude of adhesion between protein and surface, and
2. Enabling conformational modes of the protein at surface sites that maximize chemical interactions, which in turn, can affect the concentration of proteins adsorbed onto the substrate.

In addition, creation of chemically patterned surfaces can control the adsorption process by only allowing adsorption of macromolecules with a spatial arrangement that can match the substrate chemical template. Thus, by controlling the chemistry as well as texture of the surfaces, it may be possible to induce protein adsorption that would ultimately avoid conformational changes during interactions and would also allow adsorption of specific proteins having active sites oriented away from the substrate [6, 21].

Hybrid inorganic/organic composites can be designed for potential use in a wide range of medical applications. Structural diversity is achieved through control of the relative ratio of organic versus inorganic content, the chemical reaction, and the chemical composition of the

inorganic precursor molecule. In this work we obtained mesoporous silica gels with a large molar content of organic groups (up to 25%). The presence of mercaptan and amine groups in the modified gels proves that the combination of different silane agents during synthesis of the gels can satisfactorily be used to produce materials containing specifically designed chemical functionalities.

The method for preparation of hybrid silica gels developed in this work can allow incorporation of biological macromolecules throughout the gel-glass matrix since processing conditions were mild (pH was near neutral and there was no addition of alcohol). In addition, this method can also potentially allow diffusion of the molecules through the interconnected mesoporous network of the silica monoliths in a controlled, continuous way.

The foams produced in this work exhibit a hierarchical 3D structure consisting of a highly interconnected macroporous network, with a mesoporous texture. The macroporous network has the potential to allow tissue ingrowth, vascularization and nutrient delivery throughout the scaffold, which is essential for cell survival and tissue regeneration. According to the current literature the estimated pore size range for tissue ingrowth is $50\text{--}1000\text{ }\mu\text{m}$ [22].

Due to the mesoporous texture, the foams exhibit a high specific surface area, which enhances ion release from the surface and therefore the bioactivity of the foams. The mesopores also provide sites for surface reactions. As surface area increases, the number of sites available for the surface modification by mercaptan or amine groups increases (Fig. 5). Biocolonization occurs by the formation of covalent bonds between the biological macromolecules and the chemically functional groups on the surface of the foams. Therefore as surface area of the foams increases, the potential for biocolonization increases.

5. Conclusion

A sol-gel method was used to prepare mesoporous organofunctionalized silica with a large content of amine and mercaptan groups. The conventional sol-gel methods are not generally suitable for incorporation of bioactive molecules like proteins because high concentrations of alcohol and high acidity lead to denaturation of most proteins. This novel method can incorporate bioactive molecules on the porous gel-glass matrix. We also produced bioactive foams by foaming sol-gel mixtures of binary and ternary compositions. These were surface treated with amine and mercaptan groups in order that they may bond to proteins and growth factors, which can potentially enhance adhesion, differentiation and proliferation of cells. The modified foams therefore have the potential to be used as scaffolds for a wide range of tissue engineering applications, such as growing of bone or lung epithelial tissue.

Acknowledgment

The main author would like to thank CAPES for a PhD grant at Imperial College.

References

1. Y. SENUMA, S. FRANCESCHIN and J. G. HILBORN, *Biomaterials* **21** (2000) 1135.
2. M. H. SHERIDAN, L. D. SHEA, M. C. PETERS and D. J. MOONEY, *J. Control. Rel.* **64** (2000) 91.
3. L. L. HENCH, D. L. WHEELER and D. C. GREENSPAN, *J. Sol-Gel Sci. Technol.* **13** (1998) 245.
4. P. DUCHEYNE and Q. QIU, *Biomaterials* **20** (1999) 2287.
5. B. K. MANN, A. T. TSAI, T. SCOTT-BURDEN and J. L. WEST, *ibid.* **20** (1999) 2281.
6. H. S. MANSUR, W. L. VASCONCELOS, R. F. S. LENZA, R. L. ORÉFICE, E. F. REIS and Z. P. LOBATO, *J. Non-Cryst. Solids* **273** (2000) 109.
7. J. PARRADO, F. MILLAN and J. BAUTISTA, *Process Biochem.* **30** (1995) 735.
8. S. B. NICOLL, S. RADIN, E. M. SANTOS, R. S. TUAN and P. DUCHEYNE, *Biomaterials* **18** (1997) 853.
9. H. S. MANSUR, R. L. ORÉFICE, W. L. VASCONCELOS, R. F. S. LENZA and Z. P. LOBATO, *J. Int. Feder. Med. Biol. Eng.* **37** (1999) 372.
10. P. SEPULVEDA, *J. Am. Cer. Soc. Bull.* **76** (1997) 61.
11. R. F. S. LENZA and W. L. VASCONCELOS, *J. Non-Cryst. Solids* **273** (2000) 164.
12. P. SEPULVEDA, J. R. JONES and L. L. HENCH, *J. Biomed. Mater. Res.* (In press).
13. P. SARAVANAPAVAN and L. L. HENCH, *J. Biomed. Mater. Res.* **54** (2001) 608.
14. M. M. PEREIRA, A. E. CLARK and L. L. HENCH, *J. Mater. Synt. Process* **2** (1994) 189.
15. *Quantachrome Catalog-Autosorb 1*, 12/97.
16. S. BRUNAUER, I. S. DEMING, W. S. DEMING and E. TELLER, *J. Amer. Chem. Soc.* **62** (1940) 1723.
17. C. J. BRINKER and G. W. SCHERER, in "Sol-Gel Science: The Physics and Chemistry of Sol-Gel Processing" (Academic Press, San Diego, 1990) p. 907.
18. N. K. RAMAN, T. L. WARD, C. J. BRINKER, R. SEHGAL, D. M. SMITH, Z. DUAN and M. HAMPDEN-SMITH, *Appl. Catal. A General* **69** (1993) 65.
19. K. KURAOKA, Y. CHUJO and T. YAZAWA, *J. Memb. Sci.* **182** (2001) 139.
20. A. B. JEDLICKA and A. G. CLARE, *J. Non-Cryst. Solids* **28** (2001) 6.
21. D. M. LIU and I. W. CHEN, *Acta Mater.* **18** (1999) 4535.
22. S. JOSCHEK, B. NIES, R. KROTZ and A. GOPFERICH, *Biomaterials* **21** (2000) 1645.

*Received 17 August
and accepted 22 October 2001*